A HETERODYNE LASER INTERFEROMETER FOR PRIMARY CALIBRATION OF ACCELEROMETERS

Jeffrey J. Dosch
R&D Group Leader

David M. Lally
Engineering Vice President

PCB Piezotronics
Depew NY 14043

January, 2003

ABSTRACT

PCB Piezotronics has recently implemented a new A2LA accredited facility for primary calibration of accelerometers. A specially designed transfer standard was tested at the new PCB facility and at two national metrology institutes: PTB in Germany and NIST in the United States. Calibrations performed at all three facilities were found to agree to within stated uncertainties. The paper is organized as follows: primary calibration background and theory is discussed, an approach for computing displacement uncertainty in heterodyne interferometers is presented, and finally proficiency test data is compared with NIST and PTB calibrations.

NOMENCLATURE

x	Target displacement	[meter]
g	Gravity constant	[9.80665 m/s^2]
φ	Interferometer phase	[radian]
S	Sensitivity	[mV/g]
I	In-phase fringe intensity	[Volt]
Q	Quadrature fringe intensity	[Volt]
f	Calibration frequency	[Hz]
f_c	Carrier frequency	[Hz]
λ	HeNe wavelength	[632.81 nm]
u_{HeNe}	Heterodyned interferometer signal	[Volt]
u	Accelerometer output	[Volt]

INTRODUCTION

With the advent of high-resolution digital acquisition and the evolution of sophisticated test strategies, test engineers are demanding higher accuracy from their measuring equipment. For vibration applications, arguably the most important links in the measurement chain are the choice of accelerometer and the calibration of its sensitivity.

Accelerometer calibration is classified as either primary or secondary. Primary calibration can provide the highest measurement accuracy, but is more costly than secondary calibration and is thus not performed on routine or production basis. In a secondary, or comparison calibration, the unit under test (UUT) is mounted to a back-to-back working standard. Calibration is performed by comparing the output of the UUT against the output of the working standard. The working standard's sensitivity is obtained by a primary method, or more typically it is obtained through comparison to a transfer standard, where the transfer standard was calibrated by a primary method. In either case, low-uncertainty primary calibration is important for minimizing the uncertainty in the secondary calibration.

Historically, because of cost and complexity, primary calibration was performed mainly at national metrology institutes (NMI) such as NIST (National Institute of Standards and Technology) in the United States. Traceability to the NMI is maintained through a transfer standard. A calibration facility would send a primary transfer standard to the NMI for periodic calibration (annually or biannually). The primary standard is then used to calibrate the manufacturer's working standards.

Today, to meet the test engineer's demand for more accurate calibrations, accelerometer manufacturers are starting to develop the in-house ability to perform primary calibrations. There are number factors driving this: in many cases the NMI can not meet the accuracy needs of the accelerometer manufacturer; in-house primary standards can be calibrated more frequently; calibrations can be performed over frequency ranges not offered by the NMI; and back-to-back standards can be calibrated by a primary method eliminating errors introduced by the transfer standard. When a facility performs primary calibration, traceability to the NMI is ensured through the use of traceable measuring equipment and proficiency testing.

Three steps must be completed before a facility can credibly claim proficiency to perform primary calibration of accelerometers. First, the equipment and technical staff must in place. In terms of equipment, the vibration exciters are of particular importance, especially at high frequency where maintaining uniform piston-like motion free of distortion can be a challenge. Because of the exciter's importance, a considerable investment in shaker technology has been made by PCB Piezotronics. Three shakers are now used in the calibration facility: an air-bearing long stroke shaker (6 inch peak-peak) for low frequency excitation, an air bearing shaker with beryllium armature for calibration to high frequency (20 kHz), and a specially

designed air bearing shaker with alumina armature for calibration of large-size working standard accelerometers to high frequency. Second, the facility must demonstrate proficiency through comparison with a reputable NMI. In PCB's case, a transfer standard has been successfully calibrated at both PTB (Physikalisch-Technische Bundesanstalt, Germany) and NIST (United States). Finally, the organization's technical competency must be audited by an unbiased organization. In PCB's case, the primary calibration facility has been accredited to ISO/IEC 17025-1999 by the American Association of Laboratory Accreditation (A2LA).

CALIBRATION BY LASER INTERFEROMETER

In primary calibration by laser interferometery, reference motion is determined through a direct measure of the base quantities length and time. The UUT is mounted to the armature of an exciter that provides linear sinusoidal motion at a stable and known frequency *f*. UUT voltage, *u*, is measured with a precision voltmeter and armature displacement, x, is measured with a HeNe laser interferometer. UUT sensitivity is calculated as:

$$S = \frac{u}{(2\pi f)^2 x} \cdot 9.80665 \text{ [Volts/g]} \qquad (1)$$

There are number of suitable schemes for measuring armature motion using laser interferometers. A good overview of the methods can be found in ref [1]. The underlying foundation for all the methods is that HeNe laser is stable and has an accepted wavelength equal to a constant value of 632.81 nm at standard laboratory temperatures and pressures. The ISO standard organization describes three primary calibration schemes known as Methods 1, 2, and 3 [2]. Methods 1 and 2 utilize a Michelson interferometer with a single photodetector. Method 3 utilizes an interferometer with a pair of photodetector signals in quadrature.

Of the three methods, Method 1 (the fringe counting method) is simplest in concept and practice. For each interval of armature displacement equal to 1/2 a HeNe wavelength, an interferometer fringe will be produced. A fringe is detected by a photodector producing a signal that changes linearly from low to high. A precision frequency counter counts the number of fringes per excitation period, providing a measure of armature peak-to-peak displacement. Quantization of the displacement limits the usefulness of fringe counting to low frequency (less than 1000 Hz) where the armature displacement is large relative to the HeNe wavelength [2]. A second limitation of the fringe counting method is phase of the UUT cannot be determined.

The problem of fringe quantiziation can be overcome by using a quadrature detection scheme, such as Method 3, enabling interpolation of displacement between fringes and resolution equal to a small fraction of wavelength of light. In quadrature detection, two photodetector signals time-shifted by a ¼ wavelength are acquired via a PC-based digital acquisition board. The displacement is reconstructed by computing the unwrapped inverse tangent of the quadrature pair. The method has been proven accurate to high frequency (10 kHz [2]) and provides phase calibration. Over the past 10 years quadrature detection strategies have gained widespread use and acceptance for accelerometer calibration. This can be attributed, in part, to the availability of low-cost high-speed digital signal acquisition.

Both homodyne and heterodyne quadrature detection strategies have been used successfully in calibration. The interferometer described in this paper generates the quadrature pair using a heterodyne laser in conjunction with a quadrature phase demodulator. Heterodyne lasers have an advantage over homodyne lasers in that a single photodetector is required. This results in improved linearity of the quadrature pair, enabling more accurate measurement at high frequency where the armature displacement may be smaller than a fringe. Another advantage of the heterodyne approach is that the non-linearity in quadrature pair and the influence of this non-linearity on overall measurement uncertainty is easily characterized. An approach for quantifying this influence is described in this paper.

Laser interferometer technology is well established and its influence on the overall calibration uncertainty is generally small. At high frequency, calibration error is dominated by the influence of non-uniform exciter motion. The exciter must produce linear piston-like sinusoidal motion free of distortion and cross axis motion components [4]. This can be a challenge to achieve over wide frequency range and with a variety of UUTs that may range from a few grams to hundreds of grams in weight. Because of the exciter's importance, a considerable investment in improved shaker technology has been made and three shakers are now used in PCB's calibration facility: an air-bearing long stroke shaker (6 inch peak-peak) for low frequency excitation, an air bearing shaker with beryllium armature for calibration to high frequency (20 kHz), and a specially designed air bearing shaker with alumina armature for calibration of large-size working standard accelerometers to high frequency.

INTERFEROMETER THEORY

The basis for the laser interferometer is the constructive and destructive interference of two coherent light waves, one being a reference beam with a fixed path and the second beam reflected from the moving surface to be measured. Consider the reference and reflected waves in Fig 1 displaced by a distance ϕ_m. In a single pass interferometer this is related to target displacement $x(t)$ through:

$$\phi_m = 2x(t) \qquad (2)$$

Or in terms of phase between the reference and reflected waves:

$$\varphi = \frac{2\pi}{\lambda}\phi_m = \frac{4\pi}{\lambda}x(t) \qquad (3)$$

The interferometer's photodetector responds to intensity of the interfering light. The following cosine relationship between target displacement and light intensity can be derived:

$$Q = \cos\frac{4\pi}{\lambda}x(t) \qquad (4)$$

This tells us that photodetector intensity varies by the cosine of the displacement. A target displacement of ë will produce two points of maximum intensity (2 fringes). This is the basis of fringe counting methods.

In the homodyne quadrature interferometer (Fig 2) there are two photodetector signals available. The second signal is shifted optically in a ¼ wave retarder and is thus in phase quadrature to the first. Its intensity is described by the sine function:

$$I = \sin\frac{4\pi}{\lambda}x(t) \qquad (5)$$

Given a quadrature photodetector pair (Eqs. 4 and 5), the interferometer phase and target displacement can be computed:

$$\varphi(t) = \tan^{-1}\left(\frac{Q}{I}\right) \qquad (6)$$

$$x(t) = \frac{\lambda}{4\pi}\varphi(t) \qquad (7)$$

In the heterodyne quadrature interferometer only a single detector is needed (Fig 3). Interferometer phase is heterodyned on a high frequency carrier (f_c = 40MHz):

$$u_{HeNe} = \sin(2\pi f_c t + \varphi(t)) \qquad (8)$$

This is accomplished with an acousto-optic modulator (Bragg cell) which adds the carrier frequency to the reference leg of the interferometer. The heterodyned and Bragg cell signals are fed into the block marked demodulator (Fig 3). Outputs of the demodulator are the in-phase and quadrature signals I and Q. These signals are acquired by a PC-based acquisition system. Displacement is computed from Eqs. 6 and 7 in the same manner as the homodyne quadrature interferometer.

INTERFEROMETER UNCERTAINTY

The quadrature interferometer explicitly described in ref [2] is a homodyne type. An advantage of the heterodyne interferometer is the potential for smaller non- linearity in the quadrature pair. In this section a method for quantifying the heterodyne interferometer measurement uncertainty and its influence on the overall calibration uncertainty is described. This has been measured in practice and it has been found that with the heterodyne laser, errors in reading displacement are only a small part of the total uncertainty budget. Heterodyne displacement error is computed as follows.

Phase-locked test signals of 40.001 MHz and 40.000 MHz are fed into demodulator inputs RF and LO respectively (Fig 3). The RF signal simulates the heterodyned interferometer signal and the LO signal simulates carrier frequency. The chosen RF test frequency produces a Doppler shift of 1 kHz and simulates constant velocity motion of 3.16 mm/s. The RF level represents the magnitude of the photodetector output. A mirror target surface will produce a high output compared to a dull surface.

A qualitative assessment of linearity can be determined from the I vs Q Lissajous figure. A linear quadrature pair will describe a perfect circle. As the RF level is increased, the pair becomes non-linear and increasingly large deviations from a perfect circle will be observed (Fig 4). Note that RF level = 0 dBm represents an extreme case not seen in normal accelerometer calibration.

Non-linearity can be quantified by computing the measured phase from the I and Q test signals (Eq 6). Because the test signal represents a constant velocity, the true phase is known and is simply the product of velocity and time. A typical plot of the measured vs. true phase is provided in Fig 5.

The deviation of the measured phase from true phase is plotted in Fig 6. It is readily observed that the phase deviation from true is periodic. An eighth order harmonic series is fit to the data providing a mathematical expression of the phase deviation vs. true phase at a given RF level.

Once the demodulator non-linearity is known and described mathematically, it is possible to compensate for the non-linearity in software. This strategy has been used in some commercial heterodyne interferometers, and could be used to reduce the measurement uncertainty at high frequency, where displacement is equal to a fraction of a fringe. An alternative strategy is used in the PCB calibration system. When testing at high frequency a low frequency, low-amplitude displacement (equal to about 2λ to 3λ) is added to the high frequency excitation. This ensures that the measurement does not depend on a fraction of a phase cycle, greatly reducing the error influence of demodulator non-linearity.

Given the curve-fit expression for demodulator non-linearity, the displacement error attributed to this non-linearity can be computed via a simulation in Matlab® software. The simulation is performed under simulated test conditions and includes effects of sampling rate, acquisition windowing, acceleration level, and the application of low frequency displacement modulation. Results of such a simulation are given in Table 1. For comparison purposes, the "total calibration uncertainty" is included in the table. Total uncertainty is the stated uncertainty of sensitivity and includes all potential errors, e.g. interferometer, shaker distortion, meter calibration, etc. As can be seen from the table, the influence of displacement error is a small part of the total uncertainty budget.

Table 1: *Influence of demodulator non-linearity, excitation = 5 g rms.*

Excitation Frequency (Hz)	Displacement Error (%) RF=-10 dBm	Total Calibration Uncertainty (%)
100	.0002	0.2
<1500	.01	0.5
1500 to 5000	.05	1
5000 to 15000	.27	1.5

CALIBRATION EQUIPMENT

A schematic of the accelerometer calibration equipment is shown in Fig 7. The block labeled “laser” contains the HeNe laser, optics, Bragg cell, and photodectors. The laser is mounted on a granite table for isolation from environmental vibration. An air bearing shaker provides uniform distortion-free sinusoidal excitation of the accelerometer. A PC-based DAQ acquires four signals: accelerometer output, the quadrature photodetector pair I and Q, and an analog velocity signal.

Calibration of sensitivity is performed as follows. The accelerometer is excited sinusoidally at the desired frequency and amplitude level. The vibrometer, I and Q pair, and the accelerometer voltage are acquired. Displacement is determined from the I and Q photodetector pair using Eq 8. Accelerometer sensitivity is calculated using Eq 1.

A number of safegaurds are built into the calibration procedure to ensure the reasonableness of the calibration results. For example, in addition to the I and Q computation, armature acceleration is determined via an analog vibrometer. This is accomplished through the measure of the Doppler shift of the heterodyned photodetector signal using commercially available analog hardware (Polytec PI). This hardware is labeled “vibrometer controller” In Fig 6. Because of the analog electronics, the velocity signal is not a primary measurement, and thus is not used in calibration of accelerometer sensitivity. However, the vibrometer output provides a “sanity check” of sensitivity and is useful for quick analysis of an accelerometer’s frequency response. Sensitivity computed from the vibrometer and the I and Q pair generally agree to within 0.2%.

PROFICIENCY TESTING

A specially designed transfer standard, Model X353M295, was tested at PCB’s primary calibration facility, PTB in Germany, and NIST in the United States. Two proficiencies were demonstrated: top-reference measurement for calibration of “back-to-back “ working standards and base-reference measurement for calibration of transfer standards (Fig 8). In many ways the base-reference calibration is more difficult because shaker vibration modes, such as armature rocking and umbrella modes, have a greater influence on measurement error. The X353M295 utilizes an inverted element allowing both top-reference and base-reference measurements. Accelerometer specifications are provided in Table 2.

Base-reference calibration was performed at NIST at the reference frequencies of 100 Hz and 160 Hz (Table 3). NIST states a measurement uncertainty of 1% at these frequencies. The PCB and NIST calibrations were found to agree to within the NIST stated uncertainty.

PTB performed base-reference and top-reference calibrations of the transfer standard over the frequency range 5 Hz to 15 kHz. The PTB, PCB, and NIST base-reference sensitivities are plotted as a function of frequency in Fig 9 (NIST data is only at 100 Hz and 160 Hz). The PCB and PTB top-reference calibrations are plotted in Fig 10. The PTB measurement uncertainty at the 100 Hz and 160 Hz reference frequencies is only 0.2%. At the time of this writing PTB has the capability of measuring sensitivity to the lowest uncertainty of any NMI. The base-reference PCB and NIST data is compared to the PTB data in Fig 11. Over the frequency range from 5 Hz to 15 kHz, the PCB and PTB sensitivities are found to agree to within the PTB stated uncertainty. The PCB top-reference data is compared to the PTB data in Fig 12. Over the frequency range from 5 Hz to 15 kHz the sensitivities are found to agree to within the PTB stated uncertainty.

***Table 2**: X353M295 Transfer Standard*

Nominal Sensitivity	10 mV/g
Mounting	10-32 female
Sensing element	Inverted quartz shear
Power	ICP® constant current
Dynamic range	±500 g
Weight	9 grams
Case	titanium hermetic
Connector	10-32 Microdot
Mounting torque	20 inch-lb
Frequency response (±10%) Base Reference Top Reference	 0.7 Hz to 11 kHz 0.7 Hz to 20 kHz

***Table 3:** X353M295 Base-Reference Calibration, 100 and 160 Hz. Stated uncertainty in parentheses.*

Frequency (Hz)	NIST	PTB	PCB
	Sensitivity (mV/g)	Sensitivity (mV/g)	Sensitivity (mV/g)
100	10.22 (±1.0%)	10.26 (±0.2%)	10.25 (±0.2%)
160	10.19 (±1.0%)	10.26 (±0.2%)	10.26 (±0.2%)

CONCLUSION

PCB Piezotronics’ new accelerometer calibration facility, utilizing a heterodyne laser interferometer, has been accredited by A2LA. A transfer standard was tested at the new facility and at national metrology laboratories in Germany (PTB) and the United States (NIST). Calibration data at all three facilities were found to agree to within the stated uncertainties.

REFERENCES

[1] von Martens, H.J., "Current state and trends of ensuring traceability for vibration and shock measurements," Metrologia, Vol. 36, pp 357-373, 1999.

[2] ISO Standard ISO 16063-11:1999**,** Methods for the calibration of vibration and shock transducers-Part 11: Primary vibration calibration by laser interferometery.

[3] Link, A., H-J von Martens, and W. Wabinski, “New method for absolute shock calibration of accelerometers,” Proc. of SPIE, Third International Conference on Vibration Measurements by Laser Techniques,” pp. 224-235, 1998.

[4] Payne, B., “Laser Interferometer and Reciprocity Calibration of Accelerometers Using the NIST Super Shaker,” Proc. of SPIE, Third International Conference on Vibration Measurements by Laser Techniques,” pp. 187-194, 1998.

FIGURES

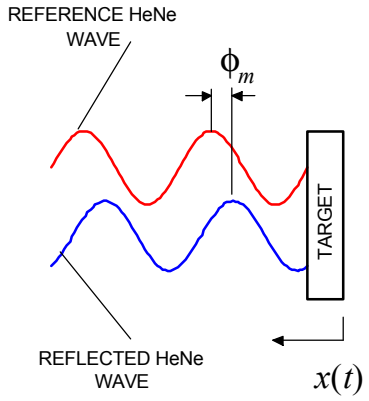

Fig 1: *Reference and reflected HeNe wave.*

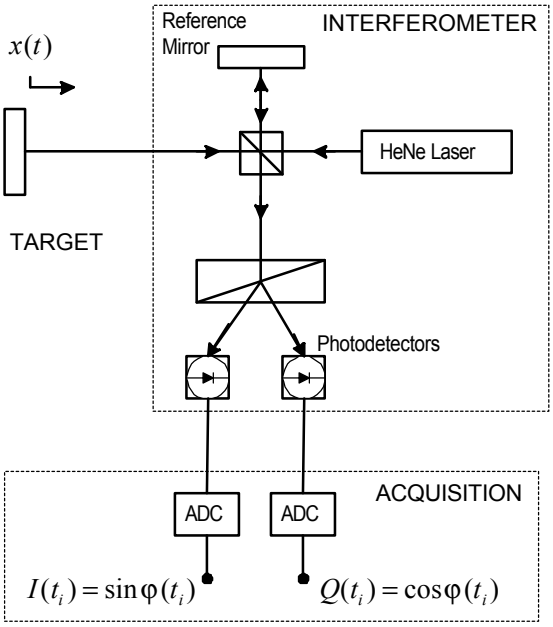

Fig 2: *Homodyne Interferometer With Quadrature Photodetector and Digital Acquisition.*

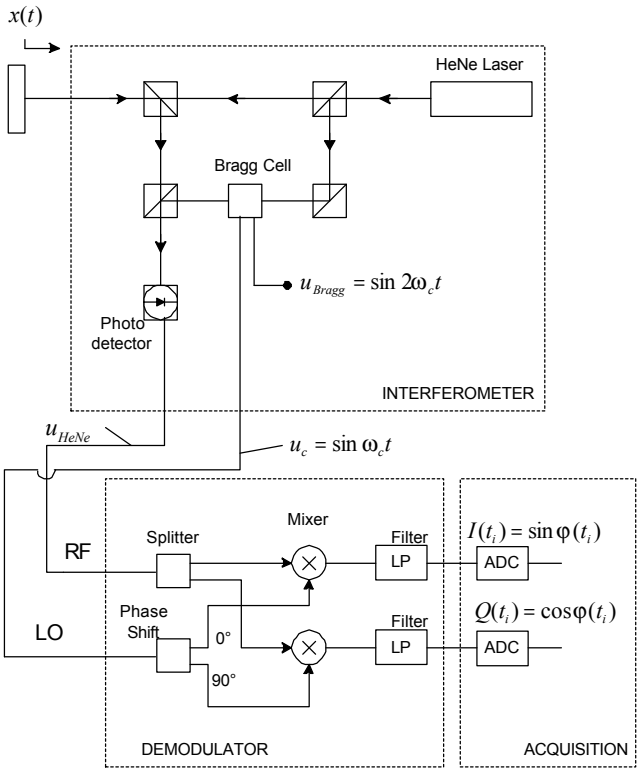

Fig 3: *Heterodyne Interferometer with Analog Quadrature Demodulation and Digital Acquisition*

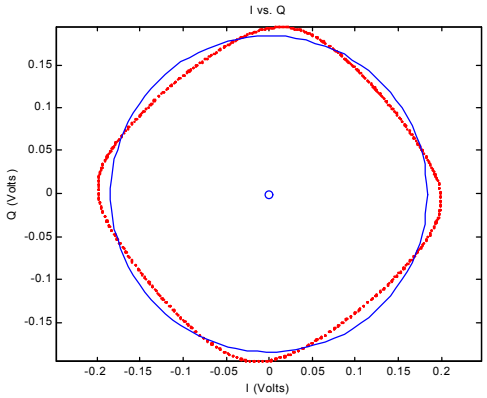

RF = 0 dBm

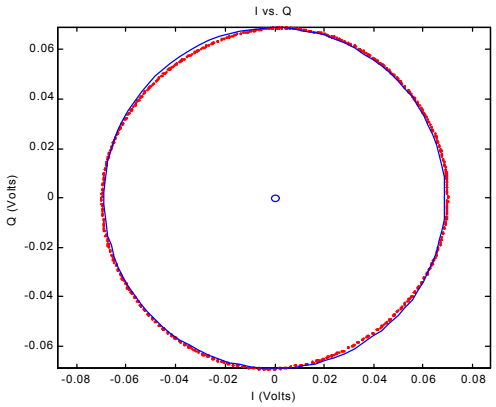

RF = -10 dBm

Fig 4: *Typical I vs Q Lissajous figure for two levels of RF.*

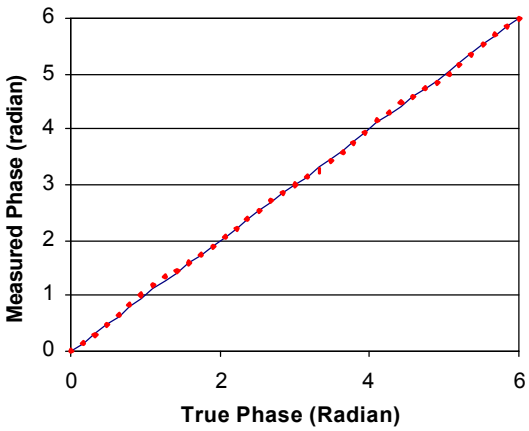

Fig 5*: Measured phase vs. true phase.*

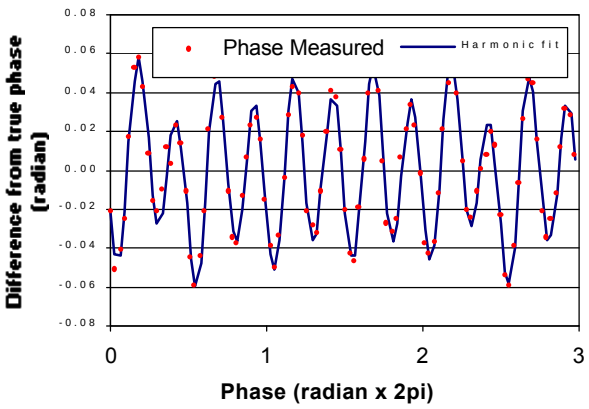

Fig 6: *Deviation from true phase.*

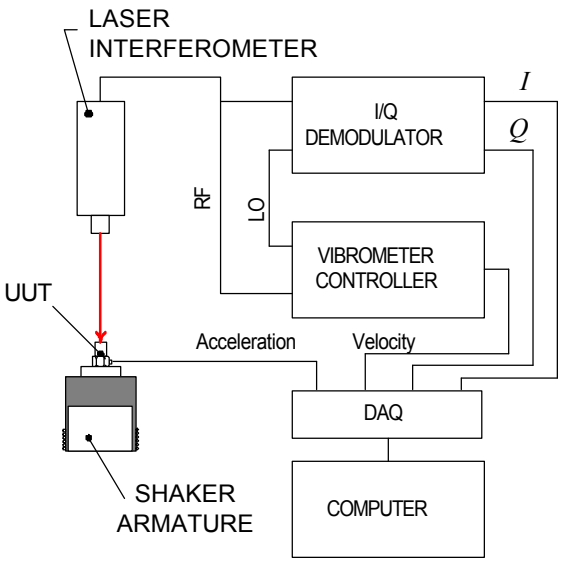

Fig 7*: Equipment for heterodyne accelerometer calibration.*

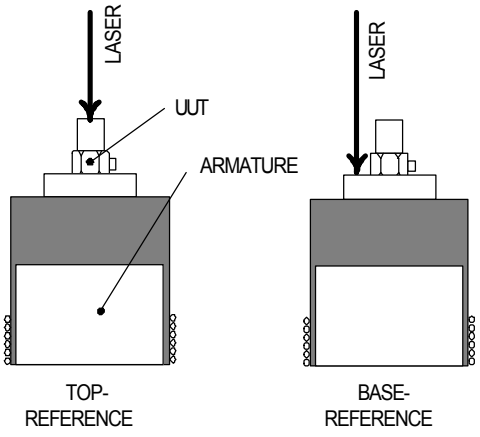

Fig 8: *Top-reference and base-reference calibration.*

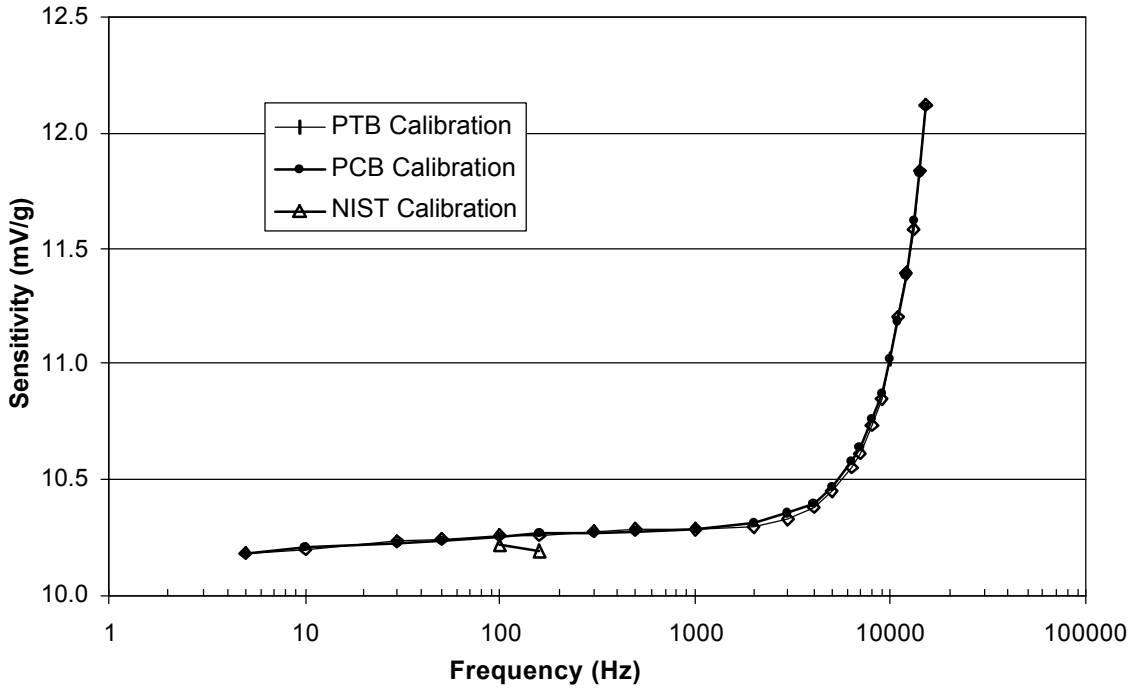

***Fig 9**: Base-reference frequency response, Model X353M295 SN 002.*

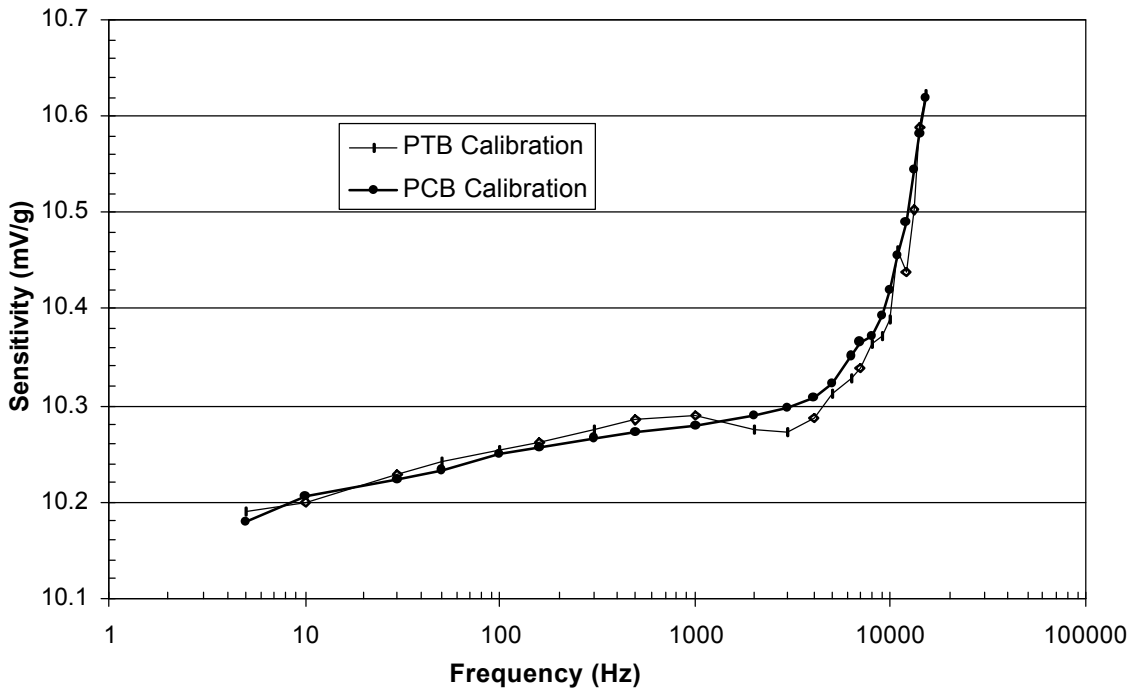

***Fig 10**: Top-reference frequency response Model X353M295 SN 002.*

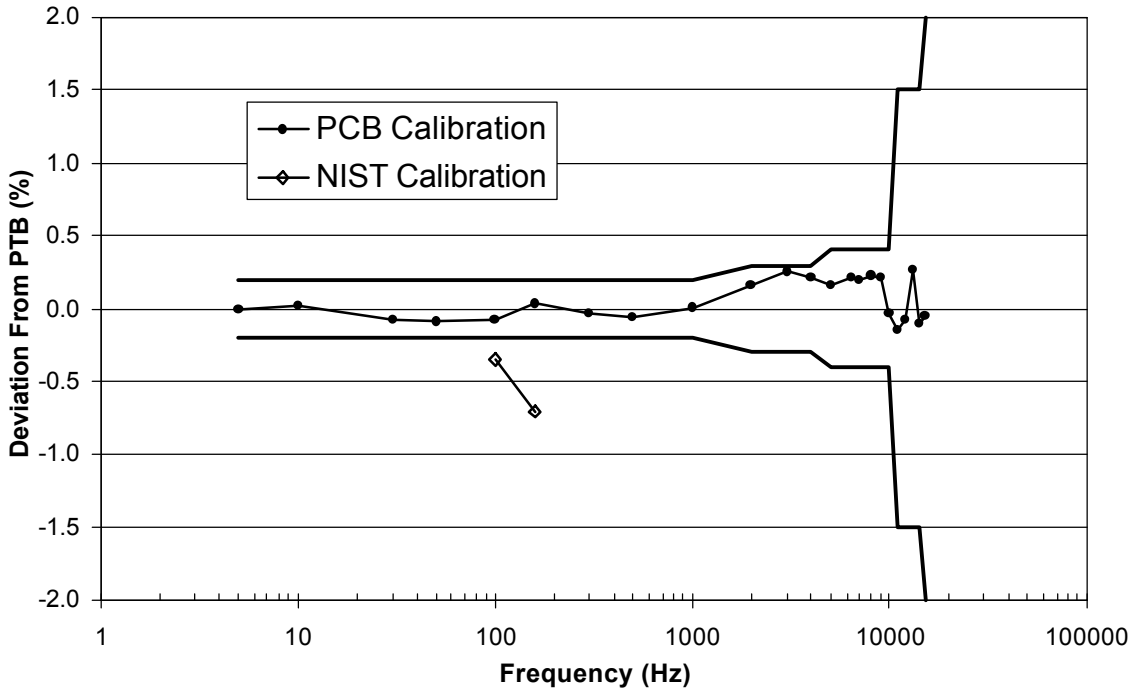

***Fig 11**: Base-reference deviation from PTB calibration data, Model X353M295 SN 002. Heavy lines indicate PTB stated uncertainty.*

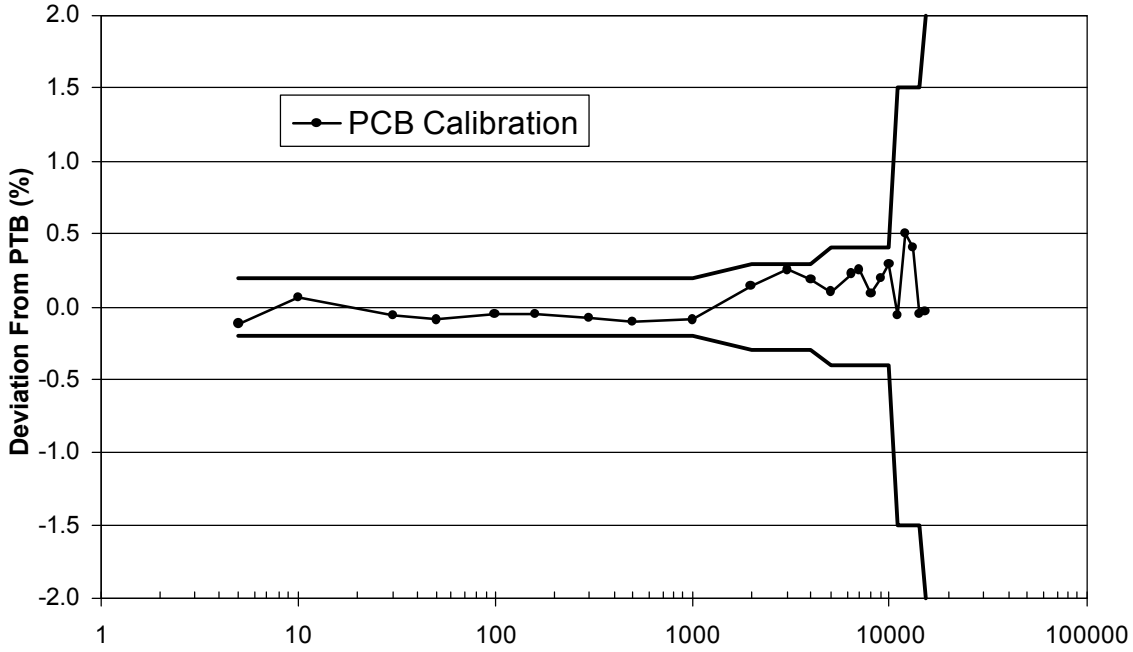

Frequency (Hz) ***Fig 12**: Top-reference deviation from PTB calibration data, Model X353M295 SN 002. Heavy lines indicate PTB stated uncertainty.*

nbn Austria GmbH
Riesstraße 146, 8010 Graz Tel. +43 316 40 28 05 | Fax +43 316 40 25 06 nbn@nbn.at | www.nbn.at